Carbon 120 (2017) 258–264

Contents lists available at ScienceDirect

Carbon

journal homepage: www.elsevier.com/locate/carbon

Graphene helicoid as novel nanospring

Haifei Zhan [a, b], Yingyan Zhang [a], Chunhui Yang [a], Gang Zhang [c, *], Yuantong Gu [b, **]

[a] School of Computing, Engineering and Mathematics, Western Sydney University, Locked Bag 1797, Penrith, NSW, 2751, Australia
[b] School of Chemistry, Physics and Mechanical Engineering, Queensland University of Technology (QUT), Brisbane, QLD, 4001, Australia
[c] Institute of High Performance Computing, Agency for Science, Technology and Research, 1 Fusionopolis Way, Singapore, 138632, Singapore

ARTICLE INFO

Article history:
Received 5 March 2017
Received in revised form
27 April 2017
Accepted 10 May 2017
Available online 13 May 2017

Keywords:
Graphene nanoribbon
Helicoid
Spring
Tensile deformation
Molecular dynamics simulation

ABSTRACT

Advancement of nanotechnology has greatly accelerated the miniaturization of mechanical or electronic devices/components. This work proposes a new nanoscale spring – a graphene nanoribbon-based helicoid (GH) structure by using large-scale molecular dynamics simulation. It is found that the GH structure not only possesses an extraordinary high tensile deformation capability, but also exhibits unique features not accessible from traditional springs. Specifically, its yield strain increases when its inner radius is enlarged, which can exceed 1000%, and it has three elastic deformation stages including the initial delamination, stable delamination and elastic deformation. Moreover, the failure of the GH is found to be governed by the failure of graphene nanoribbon and the inner edge atoms absorb most of the tensile strain energy. Such fact leads to a constant elastic limit force (corresponding to the yield point) for all GHs. This study has provided a comprehensive understanding of the tensile behaviors of GH, which opens the avenue to design novel nanoscale springs based on 2D nanomaterials.

1. Introduction

The advancement of nanotechnology has greatly accelerated the miniaturization of electronic and mechanical devices, particularly, the nanoelectromechanical system (NEMS) [1,2]. Benefited from the intriguing attributes, NEMS exhibits revolutionary functionalities which enable broad applications such as chemical and biological sensors [3], mass sensor or radiofrequency signal processing [4], drug delivery and imaging [5], and energy harvesting [6]. To facilitate various applications, NEMS is usually devised from the integration of multiple electronic and mechanical components [7], such as actuators, transistor, resonators, and motors. In this regard, nanospring is one of the simple building blocks for a variety of nanoscale devices. For instance, a nanomachine made from Pd nanospring is reported to show efficient propulsion in the presence of either magnetic or acoustic fields [8,9].

Up to date, researchers have successfully synthesized nanosprings based on different types of materials, such as Pt nanowire [10], multi-walled carbon nanotube (MWCNT) [11,12], silicon monoxide (SiO) [13], boron carbide nanowire [14], silica [15], and carbon nanocoils [16]. Meanwhile, plenty of work have been conducted to assess the electrical [17], magnetic [18], and mechanical properties of nanospring [11,19]. For instance, through atomic force microscope measurement, the MWCNT-based nanospring is found to exhibit a nonlinear response under compression [11]. An amorphous carbon nanocoil is found to have a spring constant of 0.12 N/m in the low strain region [20]. Studies show that the SiC@SiO_2 coaxial nanospring has a spring constant around 6.37 N/m [21].

It is noted that previously studied nanosprings were either made from a rod structure (i.e., nanowire) or a tube structure (i.e., nanotube), analogue to the conventional spring with similar mechanical behaviours. With the emergence of diverse 2D nanomaterials, such as graphene and transition metal dichalecogenides (TMDs, e.g., MoS_2 and WS_2), a new kind of helical structure can be synthesized through the dislocation-driven growth mechanism [22–24]. Specifically, screw dislocation can create helical planes with continuous growing surface steps, leading to atomically layered spirals [24]. A very recent work shows that the MoS_2 spiral structure can easily carry vertical current as the topology defect in the centre connects all layers and converts the vertical transport to transverse transport in the basal plane [25]. By applying voltage to the graphene-based helicoid structure, the electrical currents flow helically and thus give rise to a very large magnetic field, which bring superior inductance [24]. These intriguing properties endow the helicoid structure with appealing functionalities for usages in

* Corresponding author.
** Corresponding author.
E-mail addresses: zhangg@ihpc.a-star.edu.sg (G. Zhang), yuantong.gu@qut.edu.au (Y. Gu).

http://dx.doi.org/10.1016/j.carbon.2017.05.044
0008-6223/

nanodevices. Given the similar helicoid structures as the conventional spring, it is also of great interest to know whether they can be applied as nanosprings. Herein, by taking the graphene helicoid as a representative structure, the current work explores its tensile properties through large-scale molecular dynamics simulations. It is found that the graphene helicoid has a very large yield strain and possesses a unique tensile behavior due to the van der Waals (vdW) interactions, distinct from the conventional spring.

2. Methods

The graphene helicoid (GH) structure was constructed according to the screw dislocations as observed abundantly in annealed pyrolytic graphite [26,27]. A representative zigzag-edged structure was chosen in this work. As shown in Fig. 1, the GH was constructed through a single screw dislocation of graphene nanoribbon ($\boldsymbol{b}$, where $|\boldsymbol{b}| = 3.4$ Å) and two graphene monolayers are placed at the two ends to reduce the edge influence. Clearly, a GH structure can be defined by three parameters, i.e., the outer radius (R), inner radius (r) and turn/pitch number (N). The width and height of the GH can thus be calculated from $w = R - r$ and $h_{tot} = (N+2)|\boldsymbol{b}|$, respectively.

The study was carried out by using large-scale molecular dynamics (MD) simulations. For all simulations, the widely-used adaptive intermolecular reactive empirical bond order (AIREBO) potential was employed to describe the C–C atomic interactions [28,29]. This potential has been shown to well represent the binding energy and elastic properties of carbon materials. The cut-off distance of the AIREBO potential was chosen as 2.0 Å [30–35]. The GH structures were firstly optimized by the conjugate gradient minimization method and then equilibrated using Nosé-Hoover thermostat [36,37] for 1 ns. Free boundary conditions were applied in all three directions. To limit the influence from the thermal fluctuations, a low temperature of 1 K was adopted for all simulations. After relaxation, a constant velocity of 0.05 Å/ps was imposed on the upper end of the GH (including the upper graphene monolayer) to realize the tensile deformation (with bottom end being fixed). Note that the loading end or fixed end contains one turn of the GH together with the monolayer graphene, i.e., the deformable or effective region has $N_{eff} = N - 2$ turns. A small time step of 0.5 fs was used for all calculations with all MD simulations being performed under the software package LAMMPS [38].

3. Results and discussion

3.1. Tensile behavior

Firstly, we acquire how the GH would behave under tensile deformation. Fig. 2a illustrates the profile of the strain energy ΔE during the tensile deformation of GH (with $N_{eff} = 8$, $r \sim 7.1$ Å, and $R \sim 16.33$ Å). As expected, the GH exhibits a large tensile deformation capability with a yield strain approaching to 1500%. Note that the strain is defined as $\varepsilon = h/h_o$ (h_o and h are the initial and stretched heights of the deformable region, respectively). Evidently, the GH has four totally different deformation stages, denoted as stages I, II, III and IV, respectively. In stage I (see inset of Fig. 2b, strain from 0 to ~ 17%), the strain energy is found to increase abruptly, which is caused by the initial delamination of two adjacent nanoribbon turns. As illustrated in Fig. 2b and c, the initial delamination will create two surfaces and thus requires high strain energy to overcome the interlayer van der Waals (vdW) interactions. Simulation has further affirmed that this initial delaminating process is analogue to the tensile deformation of a multilayer graphene nanoribbon (in the out-of-plane direction). From Fig. 2b, the strain energy curve (blue line with circle markers) for the separation of a multilayer graphene nanoribbon (with same layer number as the GH) nearly overlaps with that of the GH. Thereafter, the GH undergoes a stable delamination process and the strain energy increases when the strain increases (stage II). It is worth noting that the initial delamination may not occur in a single location and the partially delaminated regions will adhere again with further stretch (see the magenta circles in Fig. 2c–f). Such process will cause small fluctuations to the strain energy curve, such as the abrupt energy fall in the enlarged view in inset of Fig. 2a. Thereafter, delaminating process will essentially concentrate in one location (Fig. 2f), and results in a smooth strain energy profile. According to Fig. 2a, the strain energy is essentially a linear function of strain in stage II, indicating that the tensile force is independent of strain. After full delamination, the GH enters the third deformation stage (Fig. 2g), which corresponds to the elastic deformation of the graphene nanoribbon and we observe a parabolic relationship between ΔE and ε (Fig. 2a). The last deformation stage (IV) corresponds to the failure of the graphene nanoribbon. Revisiting Fig. 1, the inner edge of the fully delaminated GH is a zigzag edge regularly interrupted by armchair edge. In stage IV, the crack is found to initiate at the location of armchair edge and propagate along the zigzag direction, similar deformation scenario is also reported in previous studies [39,40]. As shown in insets of Fig. 2h, monoatomic chains and pentagon carbon rings are formed at the fracture region.

Furthermore, we examine the structure of the deformed GH. It is found that the GH could fully recover to its initial state from stages I and II (see Fig. 3a). Whereas, in stage III, the graphene nanoribbon will adhere together again, but may not fully resume to its initial structure due to the local folding/flip as resulted from its low bending rigidity (see inset in Fig. 3a). Here the energy minimization is performed by removing the external tensile load from the deformed GH while keeping the other end fixed. We note that the generation of the local folding is due to the significant change of atom positions during minimization, which can be avoided if we guide the recovery process, e.g., by applying a constant velocity to compress the stretched GH. As illustrated in Fig. 3a (the dashed line), the strain energy is fully released from stage III when the GH reached its initial structure. Additionally, we have also probed the impact from the tensile load rate by considering the stretching velocity ranging from 0.02 to 0.40 Å/ps, from which we observe a uniform deformation process. As evidenced from Fig. 3b, the obtained strain energy profiles are nearly overlapped with each other, and the atomic configurations of the GH are found almost identical to each other at the same strain. Overall, these results have affirmed that the GH undergoes elastic deformation in these three stages, and can bear a large amount of tensile deformation.

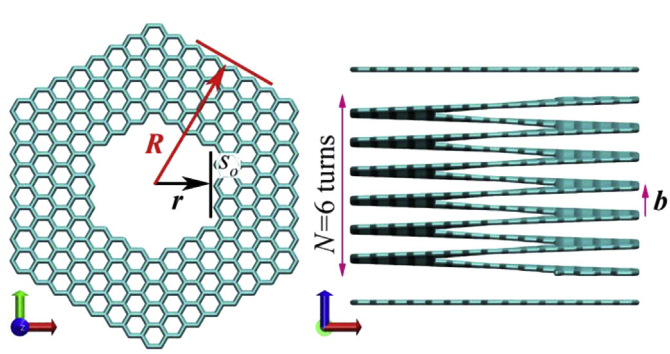

Fig. 1. Atomic structure of the GH constructed from screw dislocation, left image is top view and right image is side view. (A colour version of this figure can be viewed online.)